

# Distributed Cooperative Search Algorithm With Task Assignment and Receding Horizon Predictive Control for Multiple Unmanned Aerial Vehicles

KUN HOU<sup>1</sup>, YAJUN YANG<sup>1</sup>, XUERONG YANG<sup>2</sup>, AND JIAZHE LAI<sup>1</sup>

<sup>1</sup>Department of Aerospace Science and Technology, Space Engineering University, Beijing 101416, China

<sup>2</sup>School of Aeronautics and Astronautics, Sun Yat-sen University, Guangzhou 510275, China

Corresponding authors: Yajun Yang (yajunsand@163.com) and Xuerong Yang (yangxr23@mail.sysu.edu.cn)

This work was supported in part by the Fundamental Research Funds for the National Natural Science Foundation (NNSF) of China under Grant 61803383, and in part by the National Science Foundation for Young Scientists of China under Grant 520613.

**ABSTRACT** For target search using multiple unmanned aerial vehicles (UAVs) while knowing the probability distribution of the targets, a distributed cooperative search algorithm aiming to minimize the search time is proposed. First, an importance function for the representation of the environment is designed. Second, a mission planning system (MPS) is proposed, consisting of preliminary planning, task assignment, and post-planning layers. In the MPS, the search region is divided into a series of sub-regions of different sizes by centroidal Voronoi tessellation; these are regarded as subtasks assigned to the UAVs. The loading of the MPS improves the performance of global planning of the UAVs. Finally, receding horizon predictive control is used to plan the paths of the UAVs online. Moreover, the conflict between the requirements of target search and connectivity maintenance of the UAVs is mitigated using the minimum spanning tree strategy to optimize the communication topology while considering the communication cost when evaluating the tasks. The results of Monte Carlo simulations show that the introduction of the MPS into the traditional cooperative search framework effectively improves search and coverage efficiency.

**INDEX TERMS** Multi-UAV search, mission planning system, cooperative control, prior probability distribution.

## I. INTRODUCTION

Unmanned aerial vehicles (UAVs) are widely used in the civilian and military fields, such as for search and rescue [1], [2], environmental monitoring [3], and coordinated attacks [4]. Compared with a single UAV, multiple UAVs can complete tasks that are complex and require efficient parallel execution. Cooperative search and monitoring is one of the most important applications of multi-UAV systems. The search region is divided into numerous search cells [5]–[7], and the values of the uncertainty and the target probability associated with each cell represent the status of the environment and the distribution of the targets. The objective of the cooperative search is to find all hidden targets and cover the entire region in the shortest time.

In the cooperative search problem of multiple UAVs, the two main technical points requiring solution are the

representation of the environment and the optimal path planning of the UAVs. The probability map updated based on Bayesian estimation is a commonly used environment representation [8]–[10], and the objective of the cooperative search is the uniform convergence of the probability map. The uncertainty map is designed to guide the UAVs to reduce repeated coverage. The revisit frequency of the UAVs over each cell tends to be consistent when the swarm uses a search strategy based on the uncertainty map [11]–[13]. The above-cited research ignored the need to confirm the locations of the targets as soon as possible. To meet this need, Liu *et al.* [14] designed a revisit strategy based on a pheromone mechanism to revisit sub-areas that have a large target probability, but the algorithm fails if the probability of false alarms is relatively high.

In most research on the cooperative search problem of UAVs, the framework of the search algorithm only consists of two main modules, map update and path planning, in which the distribution and number of targets are assumed to be

The associate editor coordinating the review of this manuscript and approving it for publication was Oussama Habachi<sup>1</sup>.

unknown. When optimizing the search mission, the local optimal planning results are usually globally optimal. However, when the search importance of each cell is different, the global optimization of results obtained by local optimal planning is poor. In this study, path planning is added to a mission planning system (MPS) with three layers to reflect the importance-based search priorities of different locations in the region, which enhances the ability of global optimal planning of the UAVs.

A conventional MPS consists of two layers: task assignment and path planning. The task-assignment layer generates the assignment plan for the UAVs according to the received commands, and the path-planning layer generates the optimal paths as control commands are transmitted to the UAVs. Task-assignment algorithms can be categorized as alliance-based [15] and market-based [16], [17]. Market-based algorithms are currently favored by researchers because they have strong adaptability and no need for global communication. Market-based algorithms include contract network protocol (CNP)-based auction [18], observable Markov decision process (POMDP)-based auction [19], and random clustering auction (SCA) [20]. When a conventional MPS is applied in the dynamic environment, the path-planning layer is called frequently to optimize the task-assignment results, which consumes significant computing resources to plan useless paths. Yao *et al.* [21] improved the conventional MPS by adding a preplanning layer in which tasks are evaluated while consuming few computing resources. This improved MPS is drawn on in this study to solve the cooperative search problem of multiple UAVs, and a task-division module is designed in the preplanning layer. In the cooperative search problem, task division refers to the division of the search region into a series of sub-regions of different sizes as the subtasks of the UAVs, according to an importance function. An effective tessellation of the region is the centroidal Voronoi tessellation [22], which is an improvement of the Voronoi tessellation. It can be used to construct the coverage configuration of the UAVs by minimizing the utility function [23] and designing distributed gradient-based optimization algorithms for path planning [10], [24].

The path-planning layer aims to improve search and coverage efficiency by ensuring connectivity maintenance and collision avoidance. Many alternative methods are available for the path planning of UAVs, such as potential field [25], gradient optimization [26], reinforcement learning [27], intelligent algorithms [28], [29], the centroidal Voronoi method [10], and receding horizon predictive control [11]. In the process of path planning, conflict often occurs between task requirements and connectivity maintenance, which is a key issue requiring solution.

The main contributions of this study include the following: (1) an importance function based on the target probability and uncertainty of each cell is proposed, based on which the UAVs are guided to preferentially search areas with high target probabilities while reducing repeated coverage; (2) an MPS adapted to the cooperative search problem of the UAVs

is proposed, which improves the performance of global optimization of the system, and the number of centroidal Voronoi regions that optimizes the search efficiency is given; and (3) a control strategy ensuring connectivity maintenance and collision avoidance based on a potential field and minimum spanning tree network is advanced, which provides the largest set of constrained positions for the UAVs. The key contributions of this study are shown in Table 1.

**TABLE 1. Key contributions.**

1: The propose of importance function
2: A proper segmentation method of convex polygonal search region
3: The evaluation and reevaluation of tasks using few computing resources
4: Resolving the conflict between connectivity maintenance and task requirements by improving the communication topology of multi-UAVs

The rest of this article is organized as follows. Section 2 gives the statement and formulation of the problem as well as the preliminaries. In section 3, the framework of the distributed cooperative search algorithm is proposed, and the importance function, MPS, and receding horizon predictive control are introduced. The results of numerical simulations that verify the proposed algorithm are provided in section 4. Conclusions are summarized in section 5.

## II. PROBLEM FORMULATION AND PRELIMINARIES

### A. PROBLEM FORMULATIONS

Target search issues can be categorized as without [6], [24] or with prior information [30]. In the former, which has seen much research, the probability distribution of the targets is unknown to the UAVs, and any position of the search region is considered equally important before being searched. Comparatively little research has been conducted on search with prior information. This study aims to design a cooperative algorithm for UAVs to minimize the search time, with the nonuniform probability distribution of the targets known in advance.

Consider  $N$  UAVs ( $U_i, i = 1, 2, \dots, N$ ) equipped with airborne sensors performing a cooperative search mission in a region containing several unknown targets ( $T_j, j = 1, 2, \dots, n_T$ ) as shown in Figure 1. The multiple UAVs aim to find all latent targets and efficiently cover the entire region. For this purpose: (1) one must discretize the region and design cognitive functions to quantify the information collected by the UAVs from the environment; (2) according to the target probability, one can divide the region into a series of sub-regions of different importance, and design a task-assignment algorithm to allocate these sub-regions, or subtasks, to the UAVs; (3) a distributed control algorithm should be designed to plan optimal paths that bring the highest detection rewards to the UAVs while considering the constraints of communication maintenance and collision avoidance.

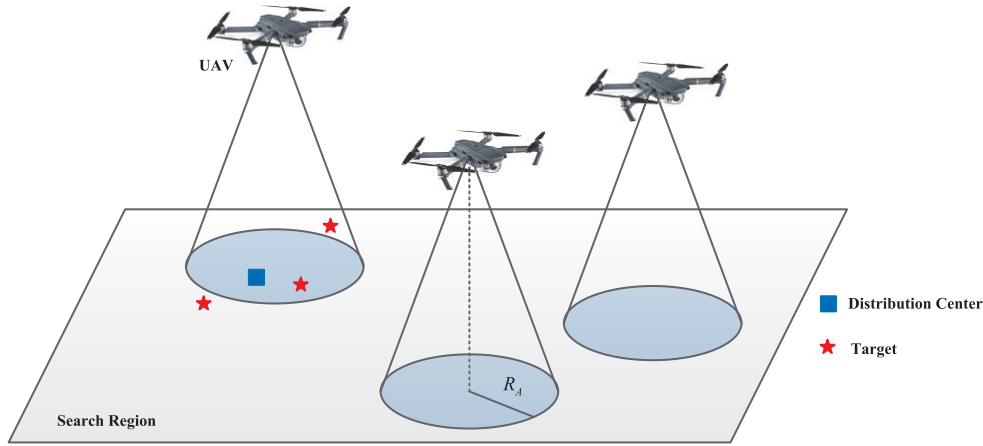


FIGURE 1. Multi-UAV cooperative search for targets.

### B. MODEL OF SEARCH ENVIRONMENT

The search region  $\Omega \in \mathbb{R}^2$  is assumed to be a rectangular plane of size  $L_x \times L_y$  in two-dimensional Euclidean space. The search region is divided into a series of grids  $\{c_p\}_{p=1}^{n_p}$  as basic search cells, of equal size  $D_x \times D_y$ . The center of cell  $c_p$  is marked  $p$  and located at  $\mu_p = [x_p, y_p]^T$ .  $\xi_p = \{0, 1\}$  indicates whether there is a target in cell  $c_p$  under the assumption that at most one target exists in a cell.

To know the prior probability distribution of the targets is significant to the UAVs searching for them. In most practical scenarios, this can be inferred by empirical models, such as rescuing people in accidents and searching for returned space capsules, in which case the targets are scattered around the vehicles or estimated landing points, which are called distribution centers. The most likely prior probability distribution of the targets is Gaussian. If  $\mu_z = [x_z, y_z]^T$  indicates the location of the distribution center, then the target probability around each center has a two-dimensional Gaussian distribution. The global target probability can be given by

$$\begin{aligned} \Pr_p &= 1 - \prod_{j=1}^{n_T} (1 - \Pr_p^j), \\ \Pr_p^j &= \frac{K_z}{\sqrt{2\pi}\sigma} \exp\left(-\frac{\|\mu_{z(j)} - \mu_p\|^2}{2\sigma^2}\right), \end{aligned} \quad (1)$$

where  $K_z$  is the gain factor corresponding to the distribution center  $\mu_z$ ,  $\sigma^2$  is the variance, and  $\|\mu_{z(j)} - \mu_p\|$  is the distance between  $p$  and the distribution center of  $T_j$ . Then,  $\Pr_p$  is the probability that at least one target exists in cell  $c_p$ .

### C. KINEMATIC MODEL AND SENSOR MODEL OF UAVS

For simplicity, the flight height of a UAV is assumed to be constant. The state of  $U_i$  can be described by  $\mathbf{X}_{i,k} = [\mu_{i,k}, \phi_{i,k}]$ , where  $\mu_{i,k} = [x_{i,k}, y_{i,k}]$  represents the coordinates and  $\phi_{i,k}$  is the heading angle at time index  $t_k$ .

The simplified kinematic model is

$$\begin{cases} \dot{x}_{i,k} = v_c \cos(\phi_{i,k}), \\ \dot{y}_{i,k} = v_c \sin(\phi_{i,k}), \\ \dot{\phi}_{i,k} = \omega_{i,k}, \\ \mu_{i,k+1} = \mu_{i,k} + [\dot{x}_{i,k}, \dot{y}_{i,k}], \\ \omega_{i,k} \leq \omega_{\max}, \end{cases} \quad (2)$$

where  $v_c$  is the constant cruising speed and  $\omega_{\max}$  is the maximum turning rate. This simplified kinematic model has been widely used [10], [24], [30] in UAV cooperative control problems. For the discrete case, the UAVs are assumed to always be located at cell centers and travel to adjacent cells within  $dT$ .

Each UAV is equipped with an optical sensor facing downward under its fuselage. With constant flight height, the circular field of view (FOV) with radius  $R_A$  of the sensor of  $U_i$  can be given by

$$\mathbb{C}_{i,k} = \{c_p \in \Omega : \|\mu_p - \mu_{i,k}\| \leq R_A\}. \quad (3)$$

### D. COMMUNICATION MODEL

Communication is the basis for the cooperation of the UAVs. The factors that are correlative to the quality of communication are complex, and include communication distance, time delay, and bandwidth. We primarily consider the effects of limited communication distance on the cooperative control of multiple UAVs. For simplicity, it is assumed that: (1) all the UAVs are homogeneous and can communicate the collected information with other UAVs; and (2) as long as the distance between any two UAVs is less than the communication distance  $R_c$ , they have an available communication link.

The network topology of multiple UAVs can be described by an undirected graph  $G(V, E(k))$ , where  $V = \{U_1, U_2, \dots, U_N\}$  is the collection of all communication nodes, and  $E(k) = \{(U_i, U_j) | \|\mu_{i,k} - \mu_{j,k}\| \leq R_c, i \neq j\}$  represents the communication links at time  $t_k$ , which are the edge sets in the graph. The second-smallest eigenvalue

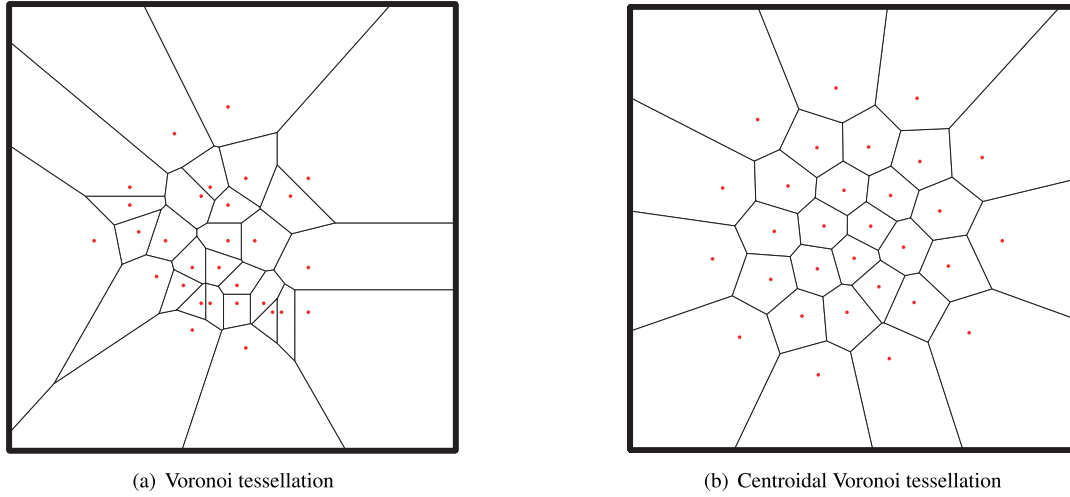


**FIGURE 2.** Difference between Voronoi tessellation and CVT.

of the Laplacian matrix  $L(k)$  is often used to indicate the connectivity of the graph. The Laplacian matrix can be calculated by

$$L(k) = D(k) - A(k), \quad (4)$$

where  $D(k)$  is the degree matrix and  $A(k)$  is the adjacency matrix, which can be expressed as

$$\begin{aligned} A(k) &= [\omega_{ij}a_{ij}]_{N \times N} \in \mathbb{R}^{N \times N}, \\ a_{ij} &= \begin{cases} 1, & \text{if } (U_i, U_j) \in E(k), \\ 0, & \text{otherwise,} \end{cases} \\ \omega_{ij} &= \exp\left(-\frac{\|\mu_{i,k} - \mu_{j,k}\|}{R_c}\right)^3, \end{aligned} \quad (5)$$

where  $a_{ij}$  indicates whether  $U_i$  and  $U_j$  are connected and  $\omega_{\max}$  is the weight of link  $(U_i, U_j)$ , which decreases with increasing  $\|\mu_{i,k} - \mu_{j,k}\|$ .

$D(k)$  can be expressed as

$$\begin{aligned} D(k) &= [d_{ij}]_{N \times N} \in \mathbb{R}^{N \times N} \\ d_{ij} &= \begin{cases} \sum_{k=1}^N \omega_{ik}a_{ik}, & \text{if } i = j, \\ 0, & \text{otherwise.} \end{cases} \end{aligned} \quad (6)$$

Then, the Laplacian matrix of the graph can be given by

$$\begin{aligned} L(k) &= [l_{ij}]_{N \times N} \in \mathbb{R}^{N \times N}, \\ l_{ij} &= \begin{cases} \sum_{k=1}^N \omega_{ik}a_{ik}, & \text{if } i = j, \\ -\omega_{ij}a_{ij}, & \text{otherwise.} \end{cases} \end{aligned} \quad (7)$$

The eigenvalues of  $L(k)$  are sorted as  $\lambda_1(k) \leq \lambda_2(k) \leq \dots \leq \lambda_N(k)$ , and  $\lambda_2(k)$  represents the algebraic connectivity. The graph is connected only if  $\lambda_2(k) > 0$ . One expects to ensure the connectivity of the network when

optimizing the communication topology, and the calculation of algebraic connectivity is helpful to verify the proposed optimization design in simulations.

#### E. CENTROIDAL VORONOI TESSELLATION

The division of the search region is a prerequisite to the task assignment of multiple UAVs. The present aim is to find a tessellation such that: (1) each sub-region is independent; (2) the target probabilities of the cells in any sub-region are relatively close; and (3) the configuration of the tessellation is related to the probability distribution of the targets.

For this purpose, the search region is first divided using a Voronoi tessellation. Also called Thiessen polygons or a Dirichlet diagram, this tessellation consists of continuous polygons formed by a set of vertical bisectors. Approaches to determine a Voronoi tessellation include divide-and-conquer algorithms, scanline algorithms, and Delaunay triangulation. Given a set of points  $\{q_g\}_{g=1}^{n_g}$ ,  $q_g \in \Omega$  with different positions as the generators, the set  $\{V_g\}_{g=1}^{n_g}$  is a Voronoi tessellation of region  $\Omega$ , and  $V_g$  is referred to as the Voronoi region corresponding to the generator  $q_g$ . For any point  $p$  in  $\Omega$ , a Voronoi region  $V_i$  has the property,

$$\|p - q_i\| \leq \|p - q_j\|, \quad i \neq j, \quad \forall p \in \Omega, \quad (8)$$

where  $q_i$  is the generator of  $V_i$ . The equality holds only if  $p$  is on the edges of  $V_i$ .

Through a Voronoi tessellation, the search region is divided into sub-regions of varying size. However, a Voronoi tessellation is completely determined by the locations of the generators. The distribution of the Voronoi regions is neither regular nor related to the target probability distribution. This requires what is called a centroidal Voronoi tessellation (CVT).

In a Voronoi tessellation, the mass centroids of  $\{V_g\}_{g=1}^{n_g}$  are  $\{z_g\}_{g=1}^{n_g}$ , and the mass centroid is generally not equivalent to the generator. However, a Voronoi tessellation can be converted to a CVT that satisfies  $q_g = z_g$ . Figure 2 shows

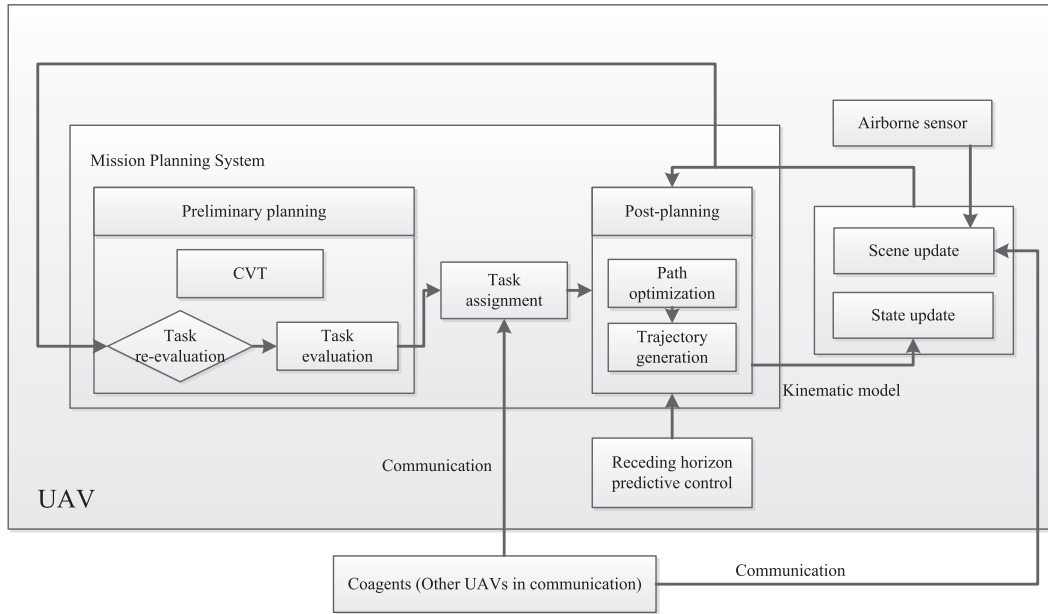


**FIGURE 3.** Framework of distributed cooperative search algorithm with task assignment and receding horizon predictive control for multi-UAVs.

the difference between a Voronoi tessellation and a CVT. It is easy to see that the distribution of the centroidal Voronoi regions is more regular than that of the Voronoi regions, the densities of the centroidal Voronoi regions are proportional to the target probabilities, and the sizes of the regions are inversely proportional to the target probabilities. Furthermore, the shape of a centroidal Voronoi region is closer to a regular polygon, which provides much convenience for a UAV to search a sub-region when its steering is restricted.

Assuming that there are  $n_g$  UAVs  $\{U_g\}_{g=1}^{n_g}$  searching the region  $\Omega$ , a tessellation  $\{V_g\}_{g=1}^{n_g}$  of  $\Omega$  can be determined using the locations of the UAVs  $\{z_g\}_{g=1}^{n_g}$  as the generators, and  $U_g$  is arranged to independently search the sub-region  $V_g$ . The search cost of a cell  $c_p$  within sub-region  $V_g$  for  $U_g$  can be defined by  $\varphi(p) = \|p - z_g\|^2$ , and the total cost function of the swarm with respect to a density function  $\rho(p)$  is defined as

$$\begin{aligned} F &= \sum_{g=1}^{n_g} \int_{p \in V_g} \rho(p) \varphi(p) dp \\ &= \sum_{g=1}^{n_g} \int_{p \in V_g} \rho(p) \|p - z_g\|^2 dp. \end{aligned} \quad (9)$$

**Lemma 1** [22]: The sufficient condition to minimize the value of  $F$  is that  $\{V_g\}_{g=1}^{n_g}$  is a Voronoi tessellation, and  $z_g$  is the mass centroid of Voronoi region  $V_g$ .

The above lemma suggests that, when using multiple UAVs to search a limited region, to place them on the generators of a CVT of the region is the least costly solution. In this study, the number of the UAVs is reduced and each UAV is made to search several centroidal Voronoi regions.

### III. ALGORITHM DESIGN

We designed a distributed cooperative search algorithm whose framework consists of two modules: mission planning and motion control. In the mission planning module, the search region is divided into a series of sub-regions as sub-tasks through a CVT, and a local auction algorithm optimally allocates the sub-tasks to the UAVs. In the motion control module, a receding horizon predictive control algorithm plans optimal paths for the UAVs to follow to search and cover the region while ensuring collision avoidance and communication between the UAVs. The framework is shown in Figure 3.

#### A. IMPORTANCE FUNCTION

An important part in the search process for the UAVs is to collect information from the environment and quantify it by different cognitive functions, which will be used to guide the UAVs to more efficiently search for targets. For example, the UAVs will preferentially search places where targets are more likely to exist based on prior target probabilities, which is a constant cognitive function under our assumptions. In addition, to discover all latent targets, the UAVs should search in different areas instead of just a certain area. An uncertainty function was designed for this purpose.

Each UAV independently searches the cells within its FOV, and the number of detections of  $U_i$  over cell  $c_p$  until time index  $t_k$  is expressed by  $H_{i,p,k} = \sum_{j=1}^k h_{i,p,k}$ , where  $h_{i,p,k}$  is the number of detections from  $t_{k-1}$  to  $t_k$ . The uncertainty function  $\eta_{i,p,k} \in [0, 1]$  quantifies the undetected information in cell  $c_p$ . The more detections that have been executed over cell  $c_p$ , the more certain is the state of  $c_p$  for  $U_i$ , and the UAVs will preferentially search places of high uncertainty. The independent update of the uncertainty function of  $U_i$  is



expressed as

$$\eta_{i,p,k} = \gamma^{h_{i,p,k}} \eta_{i,p,k-1}, \quad (10)$$

where  $\gamma \in [0, 1)$  is the decay factor determining the decreasing rate of uncertainty. The reader is referred to Sujit. [12] for details of the design of the uncertainty function.  $\eta_{i,p,k}$  decreases slower as  $H_{i,p,k}$  increases; hence repeated searches in the same area are not expected, and the UAVs must travel back and forth among different areas.

In the cooperative search mission, a swarm UAV exchanges detection information with its neighbors and uses it to update its uncertainty function. The neighbors of  $U_i$  refer to the UAVs within its communication distance, and the collection of  $U_i$  and its neighbors is  $\mathbb{N}_{i,k} = \{U_j | \|\mu_{i,k} - \mu_{j,k}\| \leq R_c, j = 1, 2, \dots, N\}$ . The joint detection result of  $U_i$  from  $t_{k-1}$  to  $t_k$  is given by  $\hat{h}_{i,p,k} = \{h_{j,p,k} | j \in \mathbb{N}_{i,k}\}$ , including its detections and the shared information of its neighbors. Based on the joint detection result, the cooperative update of the uncertainty function can be given by

$$\eta_{i,p,k} = \left( \prod_{j \in \mathbb{N}_{i,k}} \gamma_j^{h_{j,p,k}} \right) \eta_{i,p,k-1}, \quad (11)$$

where  $\gamma_j$  is the decay factor corresponding to  $U_j$ , varying with the different detection capabilities of UAVs. In the swarm consisting of homogeneous UAVs,  $\gamma_j = \gamma$  is satisfied.

To boost the priority of areas with larger target probabilities and reduce repeated searching, the importance function is designed as

$$s_{i,k,p} = \eta_{i,k,p} \text{Pr}_p. \quad (12)$$

### B. TASK ASSIGNMENT BASED ON CVT

To ensure that areas with high target probabilities are searched preferentially, the search region is divided into sub-regions of different sizes through a CVT, and these are optimally assigned to the UAVs. For this purpose, each UAV is equipped with an MPS composed of a preliminary planning layer, task-assignment layer, and post-planning layer. The preliminary planning layer generates a set of sub-regions as subtasks through a CVT, evaluates these for each UAV, and transfers the evaluations to the task assignment layer. Moreover, assigned tasks are reevaluated in this layer. The task-assignment layer generates the optimal task-assignment plan based on a distributed auction algorithm. Based on this, the post-planning layer plans optimal paths for the UAVs through the receding horizon predictive control algorithm and generates the trajectories.

CVTs are generated as follows. Deterministic approaches include Lloyd's method, the descent or gradient method, the Newton-like method, and MacQueen's method; the mathematical principles and properties of these methods have been discussed in the literature and this will not be repeated here. In this paper, Lloyd's method is selected to determine a CVT, using the following algorithm.

#### Algorithm 1 Determination Algorithm of a CVT using Lloyd's Method

**Initialization:** Discrete points  $\{q_g\}_{g=1}^{n_g}$ , density function  $\rho(p) = \text{Pr}_p$ .

**Procedure:**

1: Generate a Voronoi tessellation  $\{V_g\}_{g=1}^{n_g}$  using  $\{q_g\}_{g=1}^{n_g}$  as generators.

2: Calculate the mass centroid of  $V_g$  by  $z_g = \frac{\int_{p \in V_g} p \rho(p)}{\int_{p \in V_g} \rho(p)}$ .

3: **while**  $\frac{\sum_{g=1}^{n_g} \|z_g - q_g\|}{n_g} \geq \varepsilon$

4:     For each  $q_g$ , make  $q_g = z_g$ .

5:     Generate a new Voronoi tessellation  $\{V_g\}_{g=1}^{n_g}$ .

6:     Calculate the mass centroids  $\{z_g\}_{g=1}^{n_g}$  of  $\{V_g\}_{g=1}^{n_g}$ .

7: **end while**

In Algorithm 1, the generators are continually replaced by the centroids of the Voronoi regions. Through many iterations, the distance between the generator and centroid of the same Voronoi region is reduced dramatically. If the average distance is less than a certain threshold, then the generator and the corresponding centroid are considered coincident. Then one will obtain a CVT of the search region.

Based on Algorithm 1, the search region is divided into uniform sub-regions according to the prior target probability. The final configuration of a CVT is related to the initial positions of the generators. With the same prior target probability, the final configurations of the CVTs vary with the changes of the initial distribution of the generators. Thus the initial locations of the generators should be determined according to the target probability, so that the final configuration of a CVT reflects the target probability, as shown in Figure 4.

We next discuss how to assign and update the tasks based on the following assumptions.

- 1) The UAVs and tasks are homogeneous, so each task can be allocated to any UAV.
- 2) Tasks refer to centroidal Voronoi regions, and each can be executed repeatedly.
- 3) The execution of each task requires only one UAV.
- 4) Since evaluations of tasks are updated along with the search, each UAV keeps only one task at any moment.

A CVT of search region  $\Omega$  with  $\{q_j\}_{j=1}^{n_g}$  as the generators is  $\{V_j\}_{j=1}^{n_g}$ , and the optimization problem of searching centroidal Voronoi regions with  $N$  UAVs  $\{U_i\}_{i=1}^N$  can be expressed by

$$\max \sum_{i=1}^N \sum_{j=1}^{n_g} \alpha_{ij} R_{ij}, \quad (13)$$

where  $\alpha_{ij} = \{0, 1\}$  indicates whether task  $V_j$  is allocated to  $U_i$ , and  $R_{ij}$  is the reward that  $U_i$  can obtain by completing this

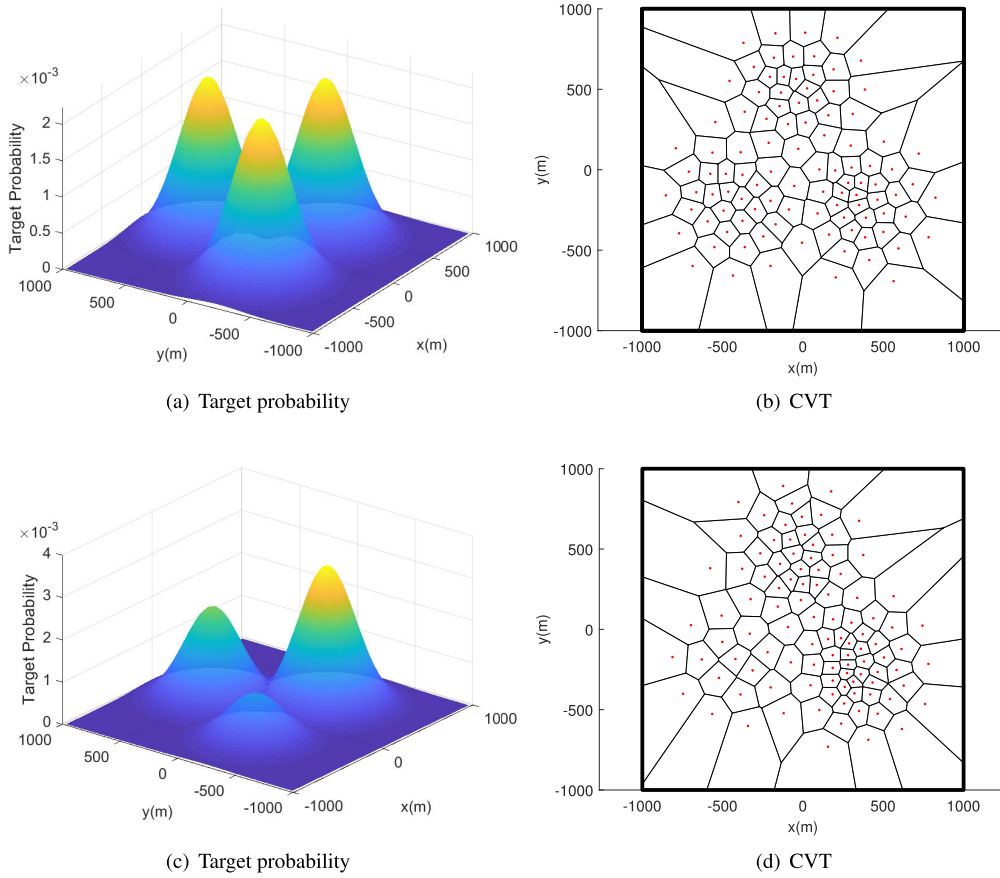


**FIGURE 4.** Centroidal Voronoi tessellations with different target probabilities; Voronoi regions are always more compact where target probabilities are larger.

task  $V_j$ . The previous assumptions can be expressed as

$$\begin{aligned} \sum_{i=1}^N \alpha_{ij} &= \{0, 1\}, \quad \forall j \in \{1, 2, \dots, n_g\}, \\ \sum_{j=1}^{n_g} \alpha_{ij} &= 1, \quad \forall i \in \{1, 2, \dots, N\}. \end{aligned} \quad (14)$$

The income is defined by  $r_{i,j,k} = \sum_{p \in V_j} s_{i,p,k}$  based on the search importance function and the cost by  $C_{i,j,k}$ . The reward is

$$R_{i,j,k} = r_{i,j,k} / C_{i,j,k}. \quad (15)$$

The cost consists of time cost  $C_{i,j,k}^t$  and communication cost  $C_{i,j,k}^c$ . The time cost consists of the arrival cost and search cost, and is defined by

$$C_{i,j,k}^t = d_{i,j,k} / \sqrt{Dx^2 + Dy^2} + \kappa S_j / S_A, \quad (16)$$

where  $d_{i,j,k} = \|\mu_{i,k} - q_j\|$  is the distance between  $U_i$  and the generator  $q_j$ ,  $S_j$  is the area of region  $V_j$ ,  $S_A$  is the area of the FOV, and  $\kappa$  is the proportionality factor related to the overlapping rate. The communication cost comes from the

risk of losing communication with other UAVs, and is defined by

$$\begin{aligned} C_{i,j,k}^c &= \sum_{l \in \tilde{N}_{i,k}} (\exp(\max(0, \frac{\|d_{l,j,k} - R'_c\|}{\|R_c - d_{l,j,k}\|})) - 1), \\ d_{l,j,k} &= \|\mu_{l,k} - q_j\|, \quad \forall U_l \in \tilde{N}_{i,k}, \end{aligned} \quad (17)$$

where  $R_c$  is the communication range, and  $R'_c < R_c$  is a custom parameter.  $\tilde{N}_{i,k} = \{U_j \mid (U_i, U_j) \in E_{MST}(k), j \neq i\}$  is the collection of other UAVs with which  $U_i$  must maintain communication links, and  $E_{MST}$  denotes the edge sets of the minimum spanning tree sub-graph  $G_{MST}$  that will be introduced in the next section. The total cost is expressed by

$$C_{i,j,k} = \beta_1 C_{i,j,k}^t + \beta_2 C_{i,j,k}^c, \quad (\beta_1, \beta_2 > 0). \quad (18)$$

The estimated comprehensive rewards of all tasks for each UAV can be evaluated by the above formulas. Based on the estimates, the task assignment is executed with a distributed auction algorithm. During the auction, each UAV bids for the task from which it can profit the most, and the auctioneer determines the ownership of each task based on all the bids. Centralized auctions are allowed in swarms with a fully connected network, and the public prices  $P_j$  of task  $V_j$  are

equal for each UAV. In practical scenarios in which networks of swarms are not fully connected, each UAV conducts a local auction with its neighbors, in which the valuation of task  $V_j$  for  $U_i$  is given by

$$e_{ij} = R_{ij} - P_{ij}, j \in \mathbb{N}_{i,k}, \quad (19)$$

where  $P_{ij}$  is the local price. For fairness, UAVs participating in a local auction should agree on the local price. The local auction algorithm is as follows.

In Algorithm 2, all UAVs are greedy bidders and will bid for every task. Once the highest bidder wins a new task, it will compare its reward to that of the task held, select the task with the larger reward, and abandon the other. Only when all tasks have been auctioned will the UAVs decide which tasks to perform.

---

**Algorithm 2** Local Auction Algorithm

---

**Initialization:** UAV  $U_i$  and the collection of UAVs within its

communication range  $\mathbb{N}_{i,k}$ , tasks  $\{V_j\}_{j=1}^{n_g}$ , estimated

rewards  $R_{i,j,k}$ , local price  $P_{i,j,k}$ , current tasks  $\{V_l^*\}_{l=1}^N$  and

corresponding rewards  $\{R_l^*\}_{l=1}^N$ , where  $U_l \in \mathbb{N}_{i,k}$ .

**Procedure:**

```

1: for  $j = 1 : n_g$ 
2:   Initial maximum evaluation  $e_{j,k}^* = 0$ 
3:   for  $U_l \in \mathbb{N}_{i,k}$ 
4:     bid  $R_{l,j,k}$ , valuation  $e_{l,j,k}$ 
5:     if  $e_{l,j,k} > e_{j,k}^*$  then
6:       assign  $V_j$  to  $U_l$ ,  $e_j^* \leftarrow e_{l,j,k}$ 
7:     end if
8:   end for
9:   the winner of  $V_j$  is  $U_q$ 
10:  if  $R_{q,j,k} > R_q^*$ 
11:    replace the current task,  $V_q^* \leftarrow V_q$ 
12:  end if
13: end for

```

---

Based on Algorithm 2, the total reward of the swarm is maximized, and the current tasks assigned are  $\{V_i^*\}_{i=1}^N$ . It is worth noting that the assignments generated by the local auction algorithms of different UAVs may conflict. Therefore, it is necessary to synchronize the task-assignment results through multi-hop communication and remove allocated tasks from the set of tasks. As the states of the UAVs and the environment update along with the search process, the preplanning layer in the MPS will be repeatedly called to reevaluate the current tasks to determine whether it is necessary to reassign tasks. The reevaluation of the current tasks includes the following two aspects: (1) the residual income of the task; and (2) cost control. Because the trajectories of UAVs searching sub-regions are not globally optimal, the remaining unsearched areas of the sub-region assigned to a UAV are scattered, and it must make a tradeoff between the residual income and search cost. The task completion  $v_i$  of  $U_i$

is defined as

$$v_i = S_i^* / S_{i,k}^A, \quad (20)$$

where  $S_i^*$  is the area of region  $V_i^*$ , and  $S_{i,k}^A$  is the area covered by  $U_i$  in  $V_i^*$  until time index  $t_k$ . The cost of the current task also changes with time, and the risk of disconnection of communication links will sharply increase the communication cost. The maximum task completion and maximum cost are defined as  $v_{\max}$  and  $C_{\max}$ , respectively, and the continuation of the current task must meet the following conditions,

$$\begin{cases} v_i \leq v_{\max}, \\ C_{i,k}^* \leq C_{\max}, \end{cases} \quad (21)$$

where  $C_{i,k}^*$  is the current cost of task  $V_i^*$  for  $U_i$ .

### C. RECEDING HORIZON PREDICTIVE CONTROL

The UAV plans its paths based on its cognition of the environment and the cognition exchanged with other UAVs, as well as the state of the swarm. Since the above information changes during the search process, the UAV must continuously replan its paths to meet the requirements of search, obstacle avoidance, and communication. Thus the path planning of the UAV is an online dynamic optimization problem, and a receding horizon predictive control algorithm is designed to solve it.

In the receding horizon predictive control algorithm, model prediction is used to solve the local optimal solution of the open-loop control in a finite-time domain, based on the current states of the UAVs and the scenario model at the sampling instant  $t_k$ . The first step of the optimal control sequence is used as the input of motion control.

The state of  $U_i$  at time index  $t_k$  is  $X_{i,k}$ , and the collection of the states of its neighbors is  $X_{i,k}^c = \{X_{j,k} | \|\mu_{i,k} - \mu_{j,k}\| \leq R_c, i \neq j\}$ . Under the assumption of constant cruising speed and flight height, the input of motion control  $u_{i,k}$  refers to the turning rate  $\omega_{i,k}$ , and the kinematic model of the UAV is  $f$ . To solve the optimal control input  $u_{i,k}^*$  through model prediction in the finite-time domain  $[t_k, t_{k+M}]$ , the benefit function of the UAV is defined as  $J_{i,k}$  and the optimization problem is expressed by

$$u_{i,k}^* = \arg \max J_i(u_{i,k}, \mathbf{X}_{i,k}, \mathbf{X}_{i,k}^c). \quad (22)$$

The following constraints should be satisfied.

$$\begin{cases} \mathbf{X}_{i,k+m} = f(\mathbf{X}_{i,k+m-1}, u_{i,k+m-1}), \\ \omega_{i,k+m} \leq \omega_{\max}, \\ m = 1, 2, \dots, M. \end{cases} \quad (23)$$

To solve the optimal path, one must first predict all possible paths. Under the constraints of the maximum turning rate and search region, the prediction of the paths based on the kinematics model of the UAV is shown in Figure 5. The possible path points at time index  $t_{k+m+1}$  are generated based on the position and heading of the UAV at time index  $t_{k+m}$ . The collection of possible path points at time index  $t_{k+m}$  is  $\tilde{w}(k+m | k)$ , and the collection of all predicted paths during the



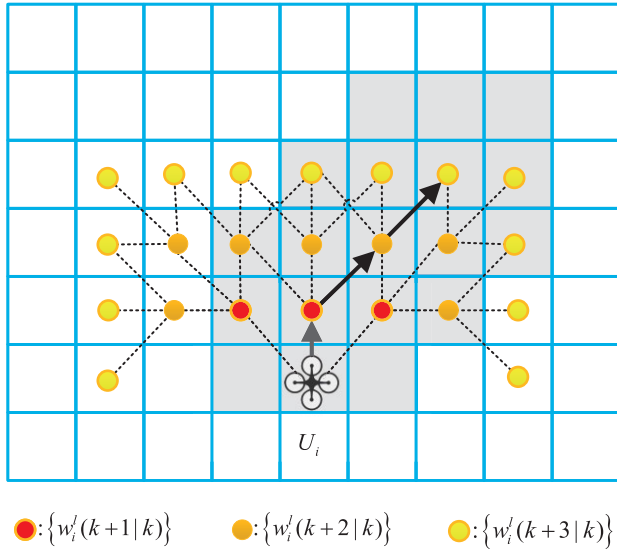


**FIGURE 5.** Illustration of three-step path prediction ( $\omega_{\max} = 45^\circ$ ); gray area represents FOV of airborne sensor.

finite-time domain  $[t_k, t_{k+M}]$  is  $\{P_i^l\}_{l=1}^{n_l}$ , where one possible path is  $P_i^l = \{w_i^l(k+1|k), w_i^l(k+2|k), \dots, w_i^l(k+M|k)\}$ ,  $M$  is the maximum number of predicted steps, and  $n_l$  is the total number of predicted paths.

The goal of path optimization is to maximize the benefit of the UAV, whose objectives include: (1) environment coverage and target search; (2) maintenance of communication; and (3) collision avoidance. The search benefit is defined as  $J^A$ , and the total expense of communication maintenance and collision avoidance is defined as  $J^B$ . The benefit function is given by

$$J_{i,l,k} = \chi_1 J_{i,l,k}^A - \chi_2 J_{i,l,k}^B, (\chi_1, \chi_2 > 0). \quad (24)$$

The UAV's main objectives include discovering all targets and covering the region. Through the task assignment, the prior detection of areas with high importance is realized. It is assumed that the target probabilities at any place in a sub-region are equivalent. For the purpose of avoiding the repeated search of the same areas, the search benefit of the UAV is represented by the uncertainty function  $\eta_{i,p,k}$  instead of the importance function  $s_{i,p,k}$ . In addition, the UAV must preferentially search the assigned sub-region, so UAV  $U_i$  will be punished if it is outside region  $V_i^*$ , and the penalty increases as the UAV travels away from the assigned region. The search benefit of  $U_i$  selecting path  $P_i^l$  is defined as

$$J_{i,l,k}^A = \delta_1 \sum_{m=1}^M \sum_{p \in \mathbb{C}_{i,k+m}} \eta_{i,p,k} - \sum_{m=1}^M \bar{\delta}_2 \exp\left(\frac{\|w_i^l(k+m|k) - q_i^*\|}{R_i^*}\right),$$

$$\bar{\delta}_2 = \begin{cases} 0, & \text{if } w_i^l(k+m|k) \in V_i^*, \\ \delta_2, & \text{else,} \end{cases}$$

$$\delta_1, \delta_2 > 0, \quad (25)$$

where  $\mathbb{C}_{i,k+m} = \{c_p \in \Omega : \|\mu_p - w_i^l(k+m|k)\| \leq R_A\}$  is the FOV of  $U_i$  located at  $w_i^l(k+m|k)$ ,  $q_i^*$  is the generator of  $V_i^*$ , and  $R_i^*$  is the circumradius of  $V_i^*$ .

To meet the needs of task assignment and information exchange between the UAVs, the communication network of the swarm must be maintained. The network of the UAV swarm is defined by the undirected graph  $G(V, E(k))$ , and the connectivity by the second smallest eigenvalue  $\lambda_2(k)$  of the Laplacian matrix  $L(k)$ , as discussed in section 2.4. Undoubtedly, a fully connected network, i.e., one with a communication link between any two UAVs, has the greatest connectivity. However, a fully connected network greatly restricts the freedom of motion of the UAVs. To achieve balance between connectivity maintenance and freedom of motion, the minimum spanning tree strategy is adopted to optimize the network topology.

A fully connected network is defined as  $G_{all}(V, E_{all}(k))$ , where  $(U_i, U_j) \in E_{all}(k)$  is satisfied for any  $i, j \in \{1, 2, \dots, N\}, i \neq j$ . A subgraph of  $G_{all}$  defined as  $G'(V, E'(k))$ , and denoted  $E' \subseteq E_{all}, G' \subseteq G_{all}$ . The Kruskal algorithm is used to generate the minimum spanning tree subgraph that meets the condition:

$$G_{MST} = \arg \min_{G' \subseteq G_{all}} \sum_{(U_i, U_j) \in E'} d_{i,j,k}, \quad (26)$$

where  $d_{i,j,k} = \|\mu_{i,k} - \mu_{j,k}\|$  is the distance between any two UAVs in the edge set  $E'$ .

**Lemma 2 [31]:** Among all subgraphs of  $G_{all}$  that guarantee connectivity, the minimum spanning tree subgraph  $G_{MST}$  provides the UAVs with the largest set of constrained positions.

As shown in Figure 6,  $\Theta_i$  indicates the communication range of  $U_i$ , the full lines represent  $E_{all}$ , and the red lines represent  $E_{MST}$ . As can be seen, in the fully connected graph, the set of constrained positions of each UAV is  $A_i = \Theta_1 \cap \Theta_2 \cap \Theta_3, i = 1, 2, 3$ , and in the minimum spanning tree

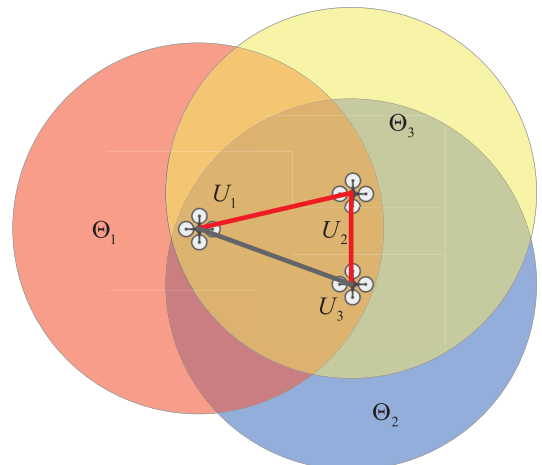


**FIGURE 6.** Set of constrained positions of UAVs in different subgraphs.

subgraph the set of constrained positions of each UAV is

$$\begin{cases} A_1 = \Theta_1 \cap \Theta_2, \\ A_2 = \Theta_1 \cap \Theta_2 \cap \Theta_3, \\ A_3 = \Theta_2 \cap \Theta_3. \end{cases} \quad (27)$$

Furthermore, it can be seen that the area of  $\Theta_i \cap \Theta_j$  increases with the decrease of the distance between  $U_i$  and  $U_j$ . By retaining the communication links in  $G_{MST}$ , the UAVs are provided with the largest set of constrained positions, while maintaining the connectivity of the network.

Since  $E_{MST}$  is composed of the shortest communication links, UAVs holding the same communication link in  $E_{MST}$  have a greater risk of collision. The artificial potential field method [25] is adopted to realize connectivity maintenance and collision avoidance, as shown in Figure 7. The current location of  $U_i$  is  $\mu_{i,k}$ , and for any other UAV  $U_j$  holding the same communication link in  $E_{MST}$  with  $U_i$ , the distance between  $U_i$  and  $U_j$  is  $d_{i,j,k}$ . To maintain connectivity and avoid collision, the distance  $d_{i,j,k}$  must be kept between  $R_c$  and  $R_s$ , where  $R_s$  is the safety distance. Given the custom parameters  $R'_c$  and  $R'_s$  that satisfy  $R_s < R'_s < R'_c < R_c$ ,  $U_i$  and  $U_j$  resist each other if the distance  $d_{i,j,k}$  is less than  $R'_s$ , and they attract each other if the distance  $d_{i,j,k}$  is greater than  $R'_c$ .  $\tilde{N}_{i,k} = \{U_j \mid (U_i, U_j) \in E_{MST}(k), j \neq i\}$  comprises the

neighbors of  $U_i$  in graph  $G_{MST}$ , and the virtual force between  $U_i$  and its neighbor  $U_j$  can be expressed by

$$F_{i,j,k} = \exp(\max(0, \frac{\|d_{i,j,k} - R'_c\|}{\|R_c - d_{i,j,k}\|})) + \exp(\max(0, \frac{\|d_{i,j,k} - R'_s\|}{\|R_s - d_{i,j,k}\|})) - 2 \quad (28)$$

The trajectory of  $U_j$  predicted by  $U_i$  with the kinematic model of the UAV in the finite-time domain  $[t_k, t_{k+M}]$  is  $\tilde{P}_j = \{\tilde{\mu}_j(k+1|k), \tilde{\mu}_j(k+2|k), \dots, \tilde{\mu}_j(k+M|k)\}$ . The expense of  $U_i$  selecting path  $P_i^l$  is defined as

$$J_{i,l,k}^B = \sum_{m=1}^M \sum_{j \in \tilde{N}_{i,k}} \tilde{F}_{i,j,k+m}^l$$

$$\tilde{F}_{i,j,k+m}^l = \exp(\max(0, \frac{\|\tilde{d}_{i,j,k+m}^l - R'_c\|}{\|R_c - \tilde{d}_{i,j,k+m}^l\|})) + \exp(\max(0, \frac{\|\tilde{d}_{i,j,k+m}^l - R'_s\|}{\|R_s - \tilde{d}_{i,j,k+m}^l\|})) - 2$$

$$\tilde{d}_{i,j,k+m}^l = \|\tilde{\mu}_j(k+m|k) - w_i^l(k+m|k)\| \quad (29)$$

Equation (29) gives the total virtual force that UAV  $U_i$  may bear when selecting path  $P_i^l$  to avoid collision and maintain connectivity. The virtual force that UAV  $U_i$  bears at time index  $t_{k+m}$  is calculated by Eq. (28) when the predicted locations of  $U_i$  and  $U_j$  are  $w_i^l(k+m|k)$  and  $\tilde{\mu}_j(k+m|k)$ . To avoid collision and maintain connectivity, a UAV will select a path in which it bears small virtual force.

#### IV. SIMULATION RESULTS

The proposed distributed cooperative search algorithm was verified based on simulation results. To achieve persuasive results, the proposed algorithm was compared with the no task-assignment and pheromone algorithms [11]. In the frameworks of the comparison algorithms, there is no task-assignment module, and UAVs using the no task-assignment algorithm tend to select paths of high importance. UAVs using the pheromone algorithm tend to select paths of high uncertainty to rapidly cover the entire region, and will be attracted by pheromones released by areas of high importance. The effects of the total number of sub-regions on the performance of search and coverage of the swarm are also analyzed.

Two indicators are proposed to quantify the coverage efficiency and search efficiency of the swarm UAVs using different search algorithms. The coverage efficiency is related to the rate of decay of global average uncertainty, and the global average uncertainty at time index  $t_k$  is

$$\bar{\eta}_k = \frac{\sum_{i=1}^N \sum_{p \in \Omega} \eta_{i,p,k}}{N n_p}. \quad (30)$$

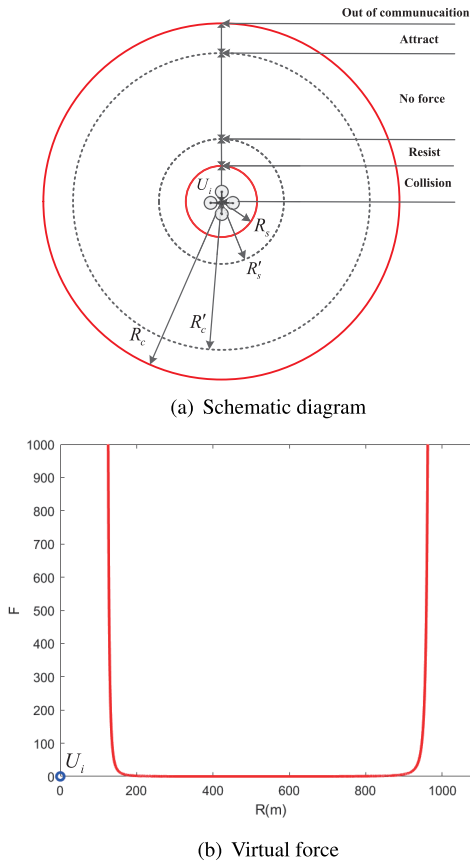
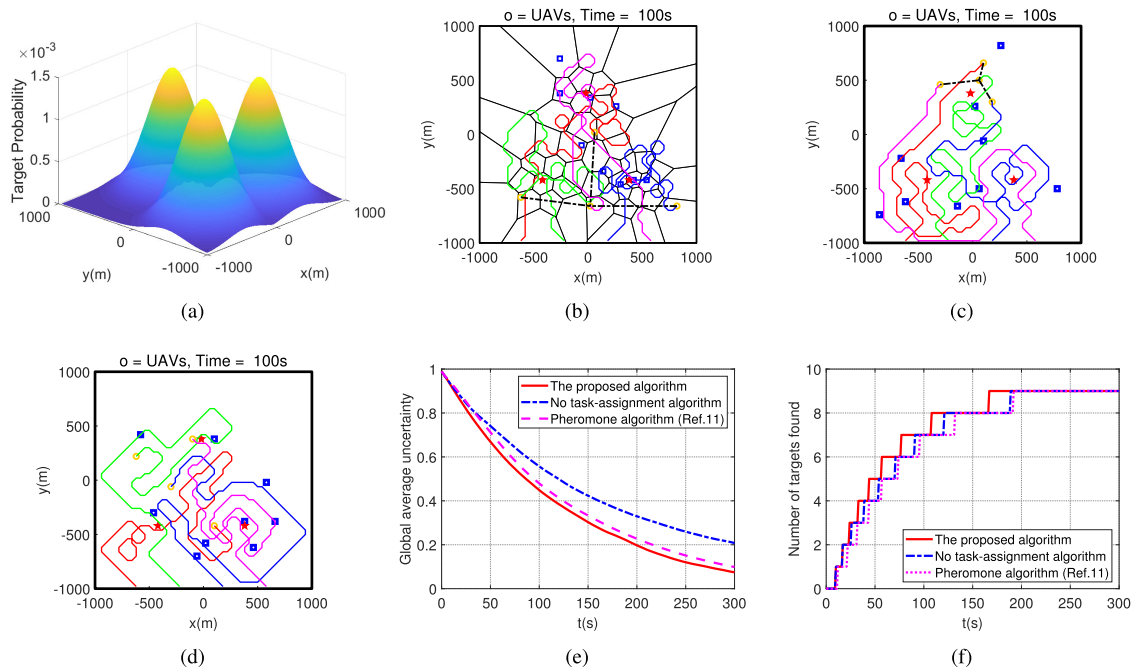


FIGURE 7. Maintaining connectivity and collision avoidance by potential field.



**FIGURE 8.** Scenario 1: (a) Target probability; (b) UAV trajectories using proposed algorithm; (c) UAV trajectories using no task-assignment algorithm; (d) UAV trajectories using pheromone algorithm; (e) comparison of global average uncertainty; (f) comparison of search efficiency.

The faster the decrease of the global average uncertainty, the higher the coverage efficiency. The search efficiency is quantified by the time used to find each target. One thousand Monte Carlo simulations were performed using the three algorithms in three scenarios, and the mean values of the time of the UAVs finding the targets and the global average uncertainty were calculated.

Simulations were conducted in a virtual square mission scenario of  $2 \text{ km} \times 2 \text{ km}$  using four UAVs, and the region was divided into 2,500 search cells of  $40 \text{ m} \times 40 \text{ m}$ . The radius of the airborne sensor's FOV was  $60 \text{ m}$  and the maximum turning rate of the UAV was  $45^\circ$ .

The communication distance  $R_c$  and safety distance  $R_h$  were  $1 \text{ km}$  and  $60 \text{ m}$ , respectively, and the corresponding custom parameters  $R'_c$  and  $R'_s$  were  $700 \text{ m}$  and  $120 \text{ m}$ . The standard deviation  $\delta$  of the Gaussian function of the target probability was  $250 \text{ m}$ . The initial value of the uncertainty function  $\eta_{i,p,0}$  of all search cells was 1 and the decay factor  $\gamma$  of all UAVs was 0.1. The four UAVs were located at  $(-620, -980)$ ,  $(-220, -980)$ ,  $(180, -980)$ , and  $(580, -980)$ , with the same heading angle of  $\pi/2$  at the outset.

Figures 8(a)–10(a) show three scenarios with different target probabilities, under which the comparison of the three algorithms was conducted. The number of targets in all three scenarios was assumed to be nine, and the number of centroidal Voronoi regions was 50. The trajectories of the UAVs using different algorithms are presented in Figures 8(b)–(d) through 10(b)–(d), where red stars represent the distribution centers, blue squares the targets, and black dotted lines the communication links in the minimum spanning tree.

The UAVs using the proposed algorithm always searched the areas near the distribution centers earlier than when using the two other algorithms.

It can be found from Figures 8(e)–10(e) and 8(f)–10(f) that the global average uncertainty of the proposed algorithm dropped faster than that of the two other algorithms most of the time, and the average time used to find each target of the swarm UAVs using the proposed algorithm was shorter than that of the two other algorithms. This means that the coverage efficiency and search efficiency of the proposed algorithm were higher than those of the others.

Compared with the no task-assignment algorithm, the MPS improved the “short sight” of the UAVs. Swarm UAVs loaded with the MPS always preferentially searched the areas with high importance, rather than seeking a local optimal solution from the neighborhood of the current locations of the UAVs. The proposed algorithm effectively improved the global optimization of the system by adding a task-assignment module above the motion-control module. Compared with the pheromone algorithm, the UAVs using the proposed algorithm divided the search region into a limited number of sub-regions, each searched independently by only one UAV, which could prevent crowding of UAVs due to the attraction of an important area. Thus each UAV could give full play to its exploration capabilities. The effects were more obvious when the targets were scattered or the areas with high target probabilities were far from the initial positions of the UAVs, as shown in scenarios 2 and 3.

The computational efficiency of the three algorithms was compared using the execution times of 1,000 sampling moments in the three scenarios, as shown in Table 1. It can be

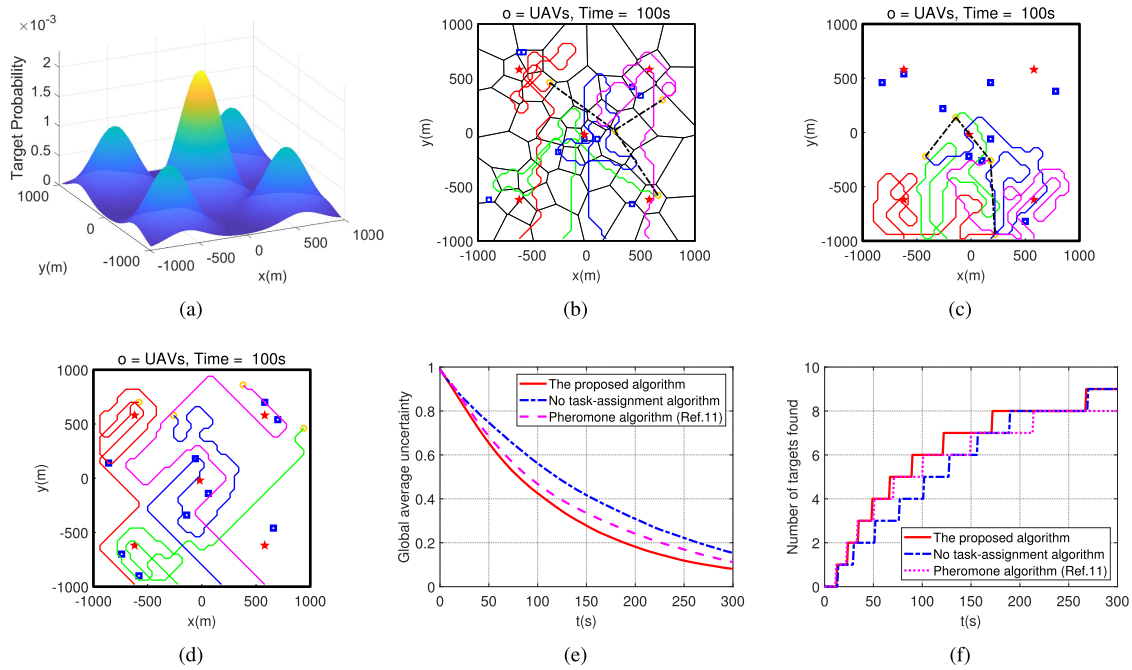


**FIGURE 9.** Scenario 2: (a) Target probability; (b) UAV trajectories using proposed algorithm; (c) UAV trajectories using no task-assignment algorithm ; (d) UAV trajectories using pheromone algorithm; (e) comparison of global average uncertainty; (f) comparison of search efficiency.

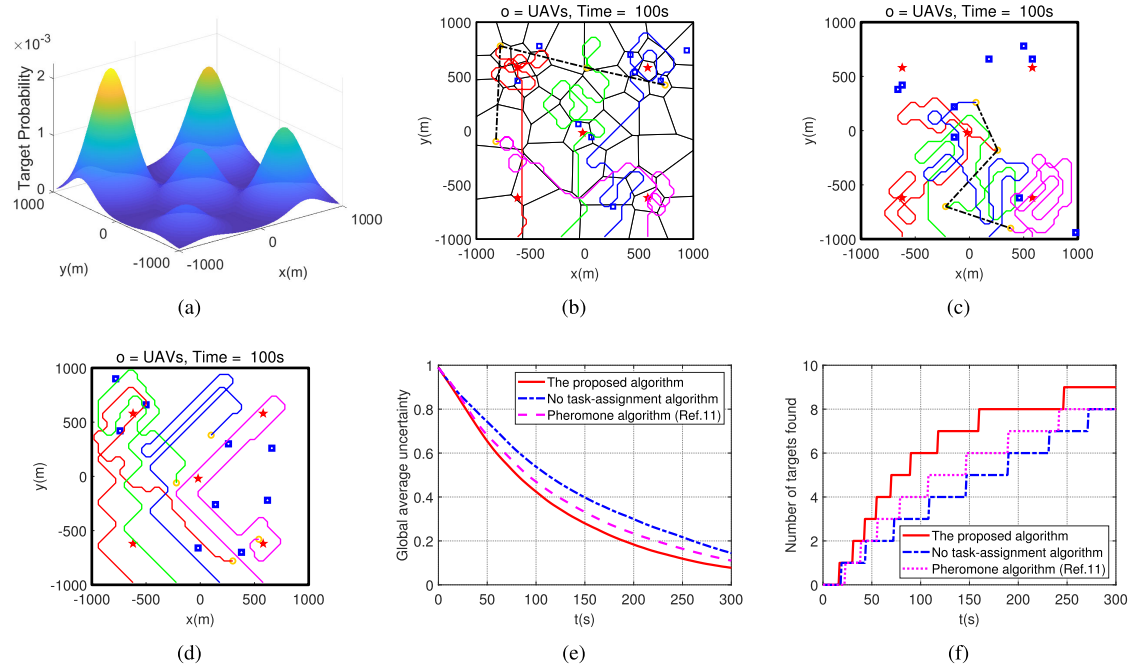


**FIGURE 10.** Scenario 3: (a) Target probability; (b) UAV trajectories using proposed algorithm; (c) UAV trajectories using no task-assignment algorithm ; (d) UAV trajectories using pheromone algorithm; (e) comparison of global average uncertainty; (f) comparison of search efficiency.

seen that due to the addition of the task-assignment module, the proposed algorithm proposed had a longer execution time, a shortcoming that must be improved in future research.

The number of centroidal Voronoi regions is the most important factor affecting the performance of the distributed

cooperative search algorithm. Based on the proposed algorithm, 10 sets of Monte Carlo simulations were performed on a swarm consisting of four UAVs with the target probability shown in Figure 9(a). The number of centroidal Voronoi regions,  $n_g$ , was set to  $\{10, 20, \dots, 90\}$ , and the number

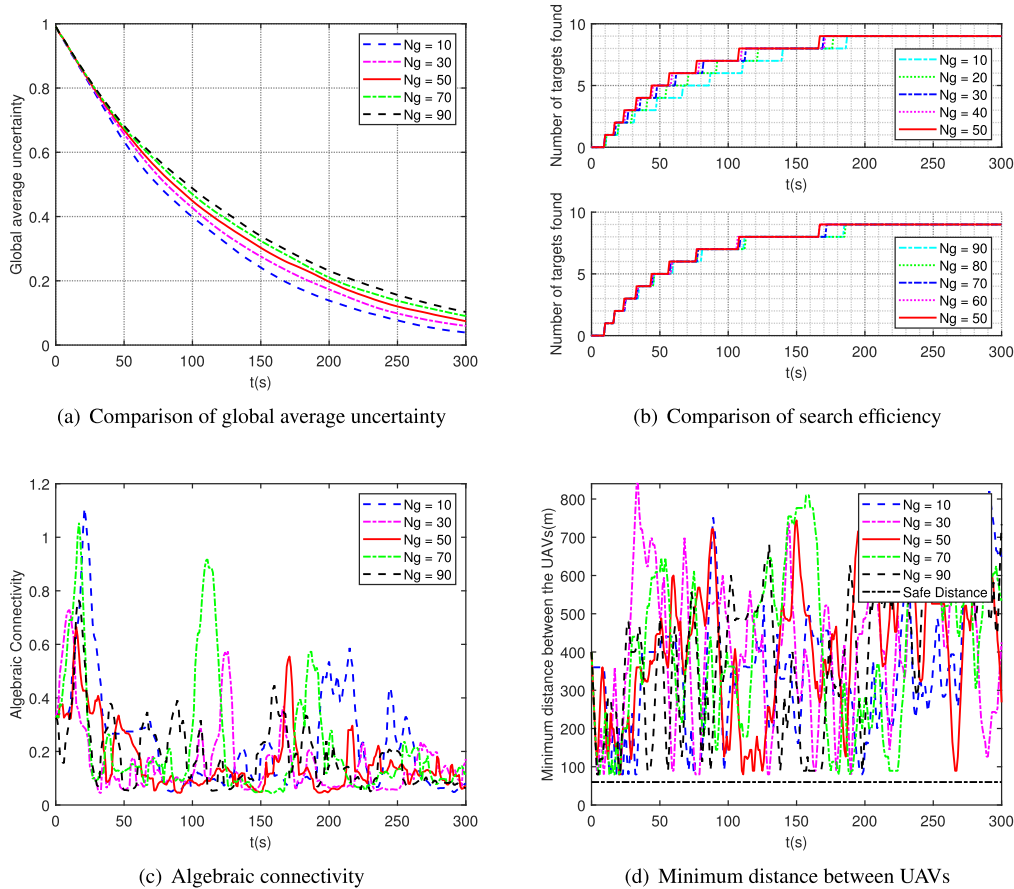


**FIGURE 11.** Effects of number of centroidal Voronoi regions on coverage efficiency and search efficiency of the swarm and validation of the strategy of communication maintenance and collision avoidance.

**TABLE 2.** Comparison of computational efficiency of the three algorithms.

Calculation time (s)	The proposed algorithm	No task-assignment algorithm	Pheromone algorithm
Scenario 1	55.32	39.82	40.44
Scenario 2	52.13	40.86	40.47
Scenario 3	48.90	37.23	37.14

of targets was assumed to be nine. The statistical results are shown in Figure 11. The effects of the number of centroidal Voronoi regions on the coverage efficiency and search efficiency of the swarm using the proposed algorithm are shown in Figures 11(a) and 11(b), respectively. As the number of centroidal Voronoi regions increased, the area of each decreased, leading to more frequent task assignments, and the probability of repeated coverage increased. The above two situations resulted in the decrease of the coverage efficiency of the swarm, but the decrease was not significant.

As can be seen in Figure 11(b), the search efficiency of the swarm first increased and then decreased as the number of centroidal Voronoi regions increased, reaching the highest

when the number was 50, as shown by the red solid line. When the number of centroidal Voronoi regions was relatively small, a large difference in the target probability still existed in different areas of the sub-region. Thus the CVT of the search region could not well reflect the distribution of the targets, which resulted in the small effect of the task assignment. When the number of centroidal Voronoi regions was too large, the coverage efficiency of the swarm decreased, and the Voronoi regions around the distribution centers were too dense, causing the difference between Voronoi regions to become insignificant, which weakened the effect of task assignment on improving the global optimization of the system.

In addition, the performance of the strategy of communication maintenance and collision avoidance was examined in the simulations, with results as shown in Figures 11(c) and 11(d), respectively. Under different numbers of centroidal Voronoi regions, the algebraic connectivity of the communication topology, i.e., the second-smallest eigenvalue of the Laplacian matrix, was always greater than zero during the search. As can be seen in Figure 11(d), the minimum distance between the UAVs was always greater than the safety distance during the search. The black dashed line represents



the safety distance between the UAVs, and there is a risk of collision if the minimum distance between the UAVs is less than the safety distance. The above results show that the strategy of communication maintenance and collision avoidance was effective for the cooperative search problem of UAVs addressed in this study.

## V. CONCLUSION

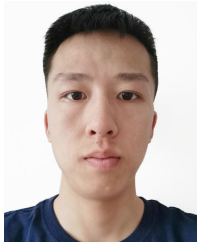
A distributed cooperative search algorithm for multiple UAVs was proposed. The representation of the environment was improved, and a task-assignment module added to the traditional cooperative search framework. Based on the proposed algorithm, the global planning capability of the system was improved, and the search efficiency of the UAV swarm in scenarios with known distribution probabilities of targets was enhanced. The proposed importance function contributed to minimizing the search time of targets and reducing repeated coverage. By dividing the search region using a centroidal Voronoi tessellation into a series of sub-regions and assigning these regions to the UAVs, the “short-sight” of the UAVs caused by the limited prediction time domain in path planning was improved. In the preplanning layer of the mission planning system (MPS), the introduction of arrival cost avoided unnecessary consumption caused by UAVs blindly pursuing high income, and the introduction of communication cost improved the conflict between mission requirements and connectivity maintenance. The minimum spanning tree strategy was applied to path planning, providing a UAV with the largest set of positions under the communication constraints. Simulation results showed that the MPS could effectively reduce the search time of targets. In addition, the optimal number of centroidal Voronoi regions that optimizes the search performance of the UAV swarm was given by the Monte Carlo method.

Inadequacy still exists in this study. A gap exists between the current hypothesis and actual scenarios. For example, the movements of UAVs are not continuous, and the influence of obstacles and ground threats on the control of the UAVs was not considered. Although the coverage efficiency and search efficiency of multiple UAVs were improved by the proposed algorithm, it increased the computational burden of UAVs. Improvements are planned for future work. In addition, the presence of false alarms in the detection results of UAVs will be considered, and the confirmation of targets requires multiple detections under this assumption.

## REFERENCES

- [1] J. Scherer, S. Yahyanejad, S. Hayat, E. Yanmaz, T. Andre, A. Khan, V. Vukadinovic, C. Bettstetter, H. Hellwagner, and B. Rinner, “An autonomous multi-UAV system for search and rescue,” in *Proc. 1st Workshop Micro Aerial Vehicle Netw., Syst., Appl. Civilian Use*, May 2015, pp. 33–38.
- [2] S. Hayat, E. Yanmaz, T. X. Brown, and C. Bettstetter, “Multi-objective UAV path planning for search and rescue,” in *Proc. IEEE Int. Conf. Robot. Autom. (ICRA)*, May 2017, pp. 5569–5574.
- [3] D. W. Casbeer, S.-M. Li, R. W. Beard, R. K. Mehra, and T. W. McLain, “Forest fire monitoring with multiple small UAVs,” in *Proc. Amer. Control Conf.*, Jun. 2005, pp. 3530–3535.
- [4] Z. Zhen, D. Xing, and C. Gao, “Cooperative search-attack mission planning for multi-UAV based on intelligent self-organized algorithm,” *Aerosp. Sci. Technol.*, vol. 76, pp. 402–411, May 2018.
- [5] Y. Yang, A. A. Minai, and M. M. Polycarpou, “Decentralized cooperative search by networked UAVs in an uncertain environment,” in *Proc. Amer. Control Conf.*, Jun. 2004, pp. 5558–5563.
- [6] J. Hu, L. Xie, J. Xu, and Z. Xu, “Multi-agent cooperative target search,” *Sensors*, vol. 14, no. 6, pp. 9408–9428, 2014.
- [7] M. Kuhlman, M. Otte, D. Sofge, and S. Gupta, “Multipass target search in natural environments,” *Sensors*, vol. 17, no. 11, p. 2514, Nov. 2017.
- [8] Y. Jin, A. A. Minai, and M. M. Polycarpou, “Cooperative real-time search and task allocation in UAV teams,” in *Proc. 42nd IEEE Int. Conf. Decis. Control*, Dec. 2003, pp. 7–12.
- [9] Y. Yang, A. A. Minai, and M. M. Polycarpou, “Evidential map-building approaches for multi-UAV cooperative search,” in *Proc. Amer. Control Conf.*, Jun. 2005, pp. 116–121.
- [10] J. Hu, L. Xie, K.-Y. Lum, and J. Xu, “Multiagent information fusion and cooperative control in target search,” *IEEE Trans. Control Syst. Technol.*, vol. 21, no. 4, pp. 1223–1235, Jul. 2013.
- [11] P. B. Sujit and D. Ghose, “Search using multiple UAVs with flight time constraints,” *IEEE Trans. Aerosp. Electron. Syst.*, vol. 40, no. 2, pp. 491–509, Apr. 2004.
- [12] P. B. Sujit and D. Ghose, “Multiple UAV search using agent based negotiation scheme,” in *Proc. Amer. Control Conf.*, Jun. 2005, pp. 2995–3000.
- [13] A. G. Shem, T. A. Mazzuchi, and S. Sarkani, “Addressing uncertainty in UAV navigation decision-making,” *IEEE Trans. Aerosp. Electron. Syst.*, vol. 44, no. 1, pp. 295–313, Jan. 2008.
- [14] Z. Liu, X. Gao, and X. Fu, “A cooperative search and coverage algorithm with controllable revisit and connectivity maintenance for multiple unmanned aerial vehicles,” *Sensors*, vol. 18, no. 5, p. 1472, May 2018.
- [15] L. E. Parker, “Adaptive heterogeneous multi-robot teams,” *Neurocomputing*, vol. 28, nos. 1–3, pp. 75–92, Oct. 1999.
- [16] B. P. Gerkey and M. J. Mataric, “Pusher-watcher: An approach to fault-tolerant tightly-coupled robot coordination,” in *Proc. IEEE Int. Conf. Robot. Autom.*, May 2002, pp. 464–469.
- [17] R. Zlot and A. Stentz, “Market-based multirobot coordination for complex tasks,” *Int. J. Robot. Res.*, vol. 25, no. 1, pp. 73–101, Jan. 2006.
- [18] B. P. Gerkey and M. J. Mataric, “Sold!: Auction methods for multirobot coordination,” *IEEE Trans. Robot. Autom.*, vol. 18, no. 5, pp. 758–768, Dec. 2002.
- [19] J. Capitan, M. T. Spaan, L. Merino, and A. Ollero, “Decentralized multi-robot cooperation with auctioned Pomdps,” *Int. J. Robot. Res.*, vol. 32, no. 6, pp. 650–671, 2013.
- [20] K. Zhang, E. G. Collins, and A. Barbu, “An efficient stochastic clustering auction for heterogeneous robotic collaborative teams,” *J. Intell. Robot. Syst.*, vol. 72, nos. 3–4, pp. 541–558, Dec. 2013.
- [21] W. Yao, N. Qi, N. Wan, and Y. Liu, “An iterative strategy for task assignment and Path planning of distributed multiple unmanned aerial vehicles,” *Aerosp. Sci. Technol.*, vol. 86, pp. 455–464, Mar. 2019.
- [22] Q. Du, V. Faber, and M. D. Gunzburger, “Centroidal Voronoi tessellations: Applications and algorithms,” *Siam Rev.*, vol. 41, no. 4, pp. 637–676, 1999.
- [23] J. Cortes, S. Martinez, T. Karatas, and F. Bullo, “Coverage control for mobile sensing networks,” *IEEE Trans. Robot. Autom.*, vol. 20, no. 2, pp. 243–255, Apr. 2004.
- [24] M. Zhang, J. Song, L. Huang, and C. Zhang, “Distributed cooperative search with collision avoidance for a team of unmanned aerial vehicles using gradient optimization,” *J. Aerosp. Eng.*, vol. 30, no. 1, Jan. 2017, Art. no. 04016064.
- [25] R. Zhou and H. Duan, “Potential field based receding horizon motion planning for centrality-aware multiple UAV cooperative surveillance,” *Aerosp. Sci. Technol.*, vol. 46, pp. 386–397, Oct. 2015.
- [26] S. K. Gan and S. Sukkarieh, “Multi-UAV target search using explicit decentralized gradient-based negotiation,” in *Proc. IEEE Int. Conf. Robot. Autom.*, May 2011, pp. 751–756.
- [27] B. Zhang, Z. Mao, W. Liu, and J. Liu, “Geometric reinforcement learning for path planning of UAVs,” *J. Intell. Robot. Syst.*, vol. 77, no. 2, pp. 391–409, Feb. 2015.
- [28] V. Roberge, M. Tarbouchi, and G. Labonté, “Comparison of parallel genetic algorithm and particle swarm optimization for real-time Uav Path planning,” *IEEE Trans. Ind. Informat.*, vol. 9, no. 1, pp. 132–141, May 2012.
- [29] J. Xin, J. Zhong, F. Yang, Y. Cui, and J. Sheng, “An improved genetic algorithm for path-planning of unmanned surface vehicle,” *Sensors*, vol. 19, no. 11, p. 2640, Jun. 2019.

- [30] X. Xiao, R. Cui, and D. Xu, "A sampling-based Bayesian approach for cooperative multiagent online search with resource constraints," *IEEE Trans. Cybern.*, vol. 48, no. 6, pp. 1773–1785, Jun. 2017.
- [31] T. Soleymani, E. Garone, and M. Dorigo, "Distributed constrained connectivity control for proximity networks based on a receding horizon scheme," in *Proc. Amer. Control Conf. (ACC)*, Jul. 2015, pp. 1369–1374.



**KUN HOU** was born in Shaanxi, China, in 1996. He received the B.E. degree in aerospace engineering from Tsinghua University, Beijing, China, in 2018. He is currently pursuing the M.E. degree in aerospace science and technology with Space Engineering University, Beijing. His current research interests include distributed swarm intelligence and the cooperative navigation and motion control of multi-UAVs.



**YAJUN YANG** received the Ph.D. degree from the National University of Defense Technology, Hunan, China, in 2016. Since 2016, he has been holding teaching appointments with Space Engineering University. He has published more than 20 articles, 11 patents, and one monograph. His current research interests include aircraft dynamics and control and the cooperative navigation and active control of UAV swarms.



**XUERONG YANG** is currently an Associate Professor and a Ph.D. Supervisor with Sun Yat-sen University, Guangzhou, China. He has published more than 40 academic articles in the field of aerospace technology, edited and translated five monographs, applied for more than 20 national invention patents, and applied for six software Copyrights. His current research interests include space system control and simulation, space system parallel test, intelligent control, and application of aerospace swarms. He has also served as a Committee Member of the Automation Institute System Simulation Committee, the Parallel Control Committee, the Command and Control Institute Space Safety Parallel System Committee, and the simulation Application Committee of the Simulation Institute.



**JIAZHE LAI** received the Ph.D. degree from the National University of Defense Technology, Institute of Electronics, Chinese Academy of Sciences, Beijing, China. He is currently an Associate Researcher with Space Engineering University. He has published more than 20 articles, six patents, and two monographs. His current research interest includes system simulation.

...